GEODYNAMICS & TECTONOPHYSICS

PUBLISHED BY THE INSTITUTE OF THE EARTH'S CRUST
SIBERIAN BRANCH OF RUSSIAN ACADEMY OF SCIENCES

2016 VOLUME 7 ISSUE 3 PAGES 459–476 ISSN 2078-502X

http://dx.doi.org/10.5800/GT-2016-7-3-0217

Paleogeodynamics

THERMODYNAMIC PROPERTIES OF ROCK-FORMING OXIDES, α-Al_2O_3, Cr_2O_3, α-Fe_2O_3, AND Fe_3O_4 AT HIGH TEMPERATURES AND PRESSURES

P. I. Dorogokupets[1], T. S. Sokolova[1], A. M. Dymshits[2], K. D. Litasov[2, 3]

[1] *Institute of the Earth's Crust, Siberian Branch of RAS, Irkutsk, Russia*
[2] *V.S. Sobolev Institute of Geology and Mineralogy, Siberian Branch of RAS, Novosibirsk, Russia*
[3] *Novosibirsk State University, Novosibirsk, Russia*

Abstract: Equations of state of corundum (α-Al_2O_3), eskolaite (Cr_2O_3), hematite (α-Fe_2O_3), and magnetite (Fe_3O_4) are constructed based on the Helmholtz free energy by simultaneous optimization of ultrasonic, X-ray diffraction, dilatometric, and thermochemical measurements. The magnetic contribution to Cr_2O_3, α-Fe_2O_3, and Fe_3O_4 Helmholtz free energy was determined via the A.T. Dinsdale model [*Dinsdale, 1991*]. The calculated thermodynamic properties of rock-forming oxides of aluminum, chromium, and iron are in good agreement with the reference data and experimental measurements at room pressure, as well as with *P-V-T* measurements at high temperatures and pressures. Thermodynamic functions (x, α, S, C_P, C_V, K_T, K_S, γ_{th}, G) of corundum, eskolaite, hematite, and magnetite are calculated at different pressures (up to 80, 70, 50 and 20 GPa, respectively) and temperatures (up to 2000 K), and the results are tabulated. The calculated Gibbs energy of rock-forming oxides can be used to construct the phase diagrams of mineral systems, which include the oxides under the conditions of the Earth's mantle.

Key words: thermodynamics; equation of state; Helmholtz free energy; oxide; corundum; eskolaite; hematite; magnetite; mantle

Recommended by E.V. Sklyarov

For citation: *Dorogokupets P.I., Sokolova T.S., Dymshits A.M., Litasov K.D.* 2016. Thermodynamic properties of rock-forming oxides, α-Al_2O_3, Cr_2O_3, α-Fe_2O_3, and Fe_3O_4 at high temperatures and pressures. *Geodynamics & Tectonophysics* 7 (3), 459–476. doi:10.5800/GT-2016-7-3-0217.

ТЕРМОДИНАМИЧЕСКИЕ СВОЙСТВА ПОРОДООБРАЗУЮЩИХ ОКСИДОВ α-Al_2O_3, Cr_2O_3, α-Fe_2O_3 И Fe_3O_4 ПРИ УСЛОВИЯХ ВЫСОКИХ ТЕМПЕРАТУР И ДАВЛЕНИЙ

П. И. Дорогокупец[1], Т. С. Соколова[1], А. М. Дымшиц[2], К. Д. Литасов[2, 3]

[1] *Институт земной коры СО РАН, Иркутск, Россия*
[2] *Институт геологии и минералогии им. В.С. Соболева СО РАН, Новосибирск, Россия*
[3] *Новосибирский государственный университет, Новосибирск, Россия*

Аннотация: На основе свободной энергии Гельмгольца построены уравнения состояния корунда (α-Al_2O_3), эсколаита (Cr_2O_3), гематита (α-Fe_2O_3) и магнетита (Fe_3O_4) путем одновременной оптимизации ультразвуковых, рентгеновских, дилатометрических данных и термохимических измерений теплоемкости при атмосферном давлении и при повышенных температурах и давлениях. Магнитный вклад в свободную энергию Гельмгольца для Cr_2O_3, α-Fe_2O_3 и Fe_3O_4 определен с помощью модели А.Т. Динсдала [*Dinsdale, 1991*]. Предложенный подход к построению уравнений состояния хорошо описывает λ-видную аномалию в теплоемкостях эс-

колаита, гематита и магнетита, которая связана с изменением магнитных свойств. Полная термодинамическая модель уравнений состояния α-Al_2O_3, Cr_2O_3, α-Fe_2O_3 и Fe_3O_4 содержит группу из семи фиксированных параметров и группу из девяти подгоночных параметров, значения которых определяются методом наименьших квадратов. Рассчитанные термодинамические функции породообразующих оксидов алюминия, хрома и железа хорошо согласуются со справочными данными и экспериментальными измерениями при атмосферном давлении, а также с современными *P-V-T* измерениями в алмазных наковальнях и многопуансонных аппаратах высокого давления. Приведена табуляция термодинамических функций (объем, коэффициент термического расширения, изобарная и изохорная теплоемкость, энтропия, адиабатический и изотермический модули сжатия, термодинамический параметр Грюнейзена и энергия Гиббса) корунда, эсколаита, гематита и магнетита до температуры 2000 К при разных давлениях (до 80, 70, 50 и 20 ГПа, соответственно). Таким образом, полученные уравнения состояния уточняют термодинамику оксидных фаз от стандартных условий до температур и давлений, соответствующих условиям мантии Земли. Рассчитанная энергия Гиббса породообразующих оксидов алюминия, хрома и железа может быть использована для построения фазовых диаграмм минеральных систем с их участием, имеющих принципиальное значение для интерпретации глобальных и промежуточных границ в земной мантии.

Ключевые слова: термодинамика; уравнение состояния; свободная энергия Гельмгольца; оксид; корунд; эсколаит; гематит; магнетит; мантия

1. Introduction

Transition-metal sesquioxides have been already studied over a wide range of temperatures and pressures as their electrical and magnetic properties are widely variable. Corundum (α-Al_2O_3), eskolaite (Cr_2O_3), hematite (α-Fe_2O_3) and iron-bearing compounds with related structures (Fe_3O_4) also play important role in the geology of the Earth interior, and ruby, $(Al,Cr)_2O_3$ was used as a pressure calibration scale for *in situ* diamond anvil cell (DAC) studies. Considering these applications, phase and magnetic transformations, as well as thermodynamic properties of corundum type oxides are of great interest both for fundamental and applied sciences.

Many experiments were conducted to study the high-pressure behavior of corundum-type compounds. It was shown that α-Al_2O_3 transforms to the Rh_2O_3(II)-type structure (space group *Pbcn*) at ~80 GPa [*Lin et al., 2004*] and to the $CaIrO_3$-type phase ("post-perovskite", space group *Cmcm*) above 130 GPa [*Oganov, Ono, 2005*; *Ito et al., 2009*]. A further phase transition to a U_2S_3-type polymorph (space group *Pnma*) at ~370 GPa [*Umemoto, Wentzcovitch, 2008*] and new thermodynamically stable compounds in the system Al-O above 330 GPa [*Liu et al., 2015*] are predicted. To date, five different crystalline polymorphs of Fe_2O_3 have been discovered and described [*Tucek et al., 2015*]. At ambient conditions, α-Fe_2O_3 crystallizes in the rhombohedral corundum-type structure (space group *R3c*). At room temperature with increasing pressure, above ~50 GPa, Fe_2O_3 forms a novel monoclinic phase with space group $P2_1/n$ and, above 67 GPa, compression triggers the transition to a different HP phase with the orthorhombic unit cell and space group *Aba*2. The pressure-induced Fe^{3+} high-spin to low-spin transition was monitored accompanying the change in the crystal structure [*Ono, Ohishi, 2005*]. At ambient pressure, both α-Fe_2O_3 and Cr_2O_3 are insulators and antiferromagnetic below the Neel temperature (T_N) of 960 and 311.5 K, respectively [*Gronvold, Samuelsen, 1975; Worlton et al., 1968*]. The electronic and magnetic properties of Cr_2O_3 under pressure were studied using a diamond anvil cell at pressures up to 55 GPa, and the evidence for two discontinuous transitions of electronic or magnetic nature, most likely associated with the change in magnetic ordering and charge transfer, were reported at ~15 to 30 GPa [*Dera et al., 2011*]. In the room-temperature compression experiment, the Cr_2O_3 remains the original rhombohedral structure up to 70 GPa [*Kantor et al., 2012*]. An orthorhombic phase was detected after heating at 30 GPa [*Shim et al., 2004*].

Magnetite (Fe_3O_4) at ambient conditions is a mixed-valence iron oxide and belongs to the spinel group of minerals and crystallizes in a cubic structure (space group *Fd3m*). At room temperature and under pressure of ~21 GPa, Fe_3O_4 transforms into distorted-cubic phase (h-Fe_3O_4) and this structure has been widely discussed. The recent *in situ* study showed that Fe_3O_4 forms a mixture of Fe_4O_5 and hematite at 9.5–11 GPa and 973–1673 K, which must recombine to distorted-cubic phase at yet higher pressures [*Woodland et al., 2012*]. A following transition of h-Fe_3O_4 into FeO and hematite assemblage and a new structural transition to orthorhombic structure (space group *Pnma*) are debated [*Ricolleau, Fei, 2016*]. The conducting and magnetic properties of magnetite were studied by different methods (Mössbauer spectroscopic, X-ray diffraction, electrical resistivity measurements), which show that Fe_3O_4 and its high-pressure polymorph are ferromag-

netic in the stability field and to at least ~70 GPa, respectively [*Shebanova, Lazor, 2003*].

The properties of corundum-type compounds have been studied under various *P-T* conditions. Calorimetric measurements of enthalpies of formation are reported in [*Moore, Kelley, 1944; Gronvold, Westrum, 1959; Westrum, Gronvold, 1969; Gronvold, Sveen, 1974; Gronvold, Samuelsen, 1975; Goto et al., 1989; et al.*]. Results of the theoretical studies of elastic properties, crystal structure, thermodynamics and stability of corundum-type oxides are presented in [*Sivasubramanian et al., 2001; Wessel, Dronskowski, 2013*]. Heat capacities at ambient pressure of α-Al_2O_3, Cr_2O_3, α-Fe_2O_3, and Fe_3O_4 [*Hemingway, 1990; Klemme et al., 2000; Gurevich et al., 2009; Snow et al., 2010*] and thermal expansion [*Wachtman, 1962; Schauer, 1965; Skinner, 1966; White, Roberts, 1983; Aldebert, Traverse, 1984; Hill et al., 2010; Dymshits et al., 2016; et al.*] were studied experimentally in detail. Elastic properties of α-Al_2O_3, Cr_2O_3, α-Fe_2O_3, and Fe_3O_4 were experimentally studied as a function of *P* and *T* using X-ray diffraction and ultrasonic technique [*Wilburn et al., 1978; Sato, Akimoto, 1979; Finger, Hazen, 1980; Nakagiri et al., 1986; Richet et al., 1998; Dubrovinsky et al., 1998; Kim-Zajonz et al., 1999; Grevel et al., 2000; Reichmann, Jacobsen, 2004; Gatta et al., 2007; Dera et al., 2011; Kantor et al., 2012; Dewaele, Torrent, 2013*; *Dymshits et al., 2016*], and their more detailed description is provided below (see section 3 and 4).

Based on the current experimental results, an internally consistent set of thermochemical and thermophysical data can be consolidated. The thermodynamic analysis can provide internal consistency of different types of physical property measurements and give the complete set of data on a system, for example, based on the Helmholtz free energy. The aim of this paper is to set up the equations of state (EoS) of α-Al_2O_3, Cr_2O_3, α-Fe_2O_3, and Fe_3O_4 and calculate the full set of thermodynamic functions depending on temperature and pressure.

2. Thermodynamic model of EoS

The proposed thermodynamic model of equations of state of corundum, eskolaite, hematite, and magnetite is based on a modified formalism from our previous studies [*Dorogokupets et al., 2012, 2014, 2015; Sokolova et al., 2013, 2016*] and takes into account the magnetic contribution.

The Helmholtz free energy of sesquioxides in classical form [*Zharkov, Kalinin, 1971*]:

$$F(V,T) = U_0 + E_0(V) + F_{th}(V,T) - F_{th}(V,T_0) + F_{anh}(V,T) - F_{anh}(V,T_0) + F_{mag}(T) - F_{mag}(T_0), \quad (1)$$

where U_0 is the reference energy; $E_0(V)$ is the potential part of the Helmholtz free energy on reference isotherm T_0=298.15 K, which depends only on volume; $F_{th}(V,T)$ is the thermal part of the Helmholtz free energy, which depends on volume and temperature; $F_{anh}(V,T)$ is the contribution of intrinsic anharmonicity to the Helmholtz free energy, which depends on volume and temperature; and $F_{mag}(T)$ is the magnetic contribution to the Helmholtz free energy, which depends only on temperature.

In physics of metals, a potential part of free energy is often described using the well-known Vinet equation [*Vinet et al., 1987*], which defines the potential components of EoS $E_0(V)$, $P_0(V)$, $K_{T0}(V)$, and K_0' depending on volume, as:

$$E_0(V) = 9K_0V_0\eta^{-2}(1 - [1 - \eta(1 - y)]\exp[(1 - y)\eta]), \quad (2.1)$$

$$P_0(V) = 3K_0y^{-2}(1 - y)exp[(1 - y)\eta], \quad (2.2)$$

$$K_{T0}(V) = K_0y^{-2}[1 + (\eta y + 1)(1 - y)]\exp[(1 - y)\eta], \quad (2.3)$$

$$K_0' = \frac{1}{3}\left[2 + y\eta + \frac{y(1-\eta)+2y^2\eta}{1+(1-y)(1+y\eta)}\right], \quad (2.4)$$

where $y=(V/V_0)=x^{1/3}$, and $\eta=1.5(K_0'-1)$.

As shown earlier [*Dorogokupets, Dewaele, 2007; Dorogokupets, 2010*], thermodynamic functions at temperatures above the reference isotherm (>298.15 K) can be calculated using the Debye or Einstein model. For a more accurate calculation of standard entropy, we use the Einstein model with two characteristic temperatures. The thermal part of the Helmholtz free energy is expressed as a sum of two Einstein temperature contributions and the contribution of intrinsic anharmonicity:

$$F_{th}(V,T) = m_1 RT\ln\left(1-\exp\frac{-\Theta_1}{T}\right) + m_2 RT\ln\left(1-\exp\frac{-\Theta_2}{T}\right) + \left(-\frac{3}{2}n\mathrm{R}a_0 x^m T^2\right), \tag{3}$$

where Θ_1 и Θ_2 are characteristic temperatures depending only on volume; $m_1+m_2=3n$, n is number of atoms in a chemical formula of compound; a_0 is an intrinsic anharmonicity parameter; m is an anharmonic analogue of the Grüneisen parameter; R the gas constant (R=8.31451 Jmol^{-1}K^{-1}).

Hereafter, for simplicity, let us limit ourselves to one characteristic temperature Θ_i (i=1, 2). Differentiating eq. (3) with respect to temperature at constant volume, we obtain entropy, and calculate internal energy:

$$S = -\left(\frac{\partial F_{th}}{\partial T}\right)_V = 3n\mathrm{R}\left[-\ln\left(1-\exp\frac{-\Theta_i}{T}\right) + \frac{\Theta_i/T}{\exp(\Theta_i/T)-1}\right] + 3nRa_0x^mT, \tag{4}$$

$$E_{th} = F_{th} + TS = 3n\mathrm{R}\left[\frac{\Theta_i}{\exp(\Theta_i/T)-1}\right] + \frac{3}{2}nRa_0x^mT^2. \tag{5}$$

Differentiating eq. (3) with respect to volume at constant temperature, we determine the thermal part of pressure:

$$\mathrm{P_{th}} = -\left(\frac{\partial \mathrm{F_{th}}}{\partial \mathrm{V}}\right)_\mathrm{T} = 3\mathrm{nR}\frac{\gamma}{\mathrm{V}}\left[\frac{\Theta_\mathrm{i}}{\exp(\Theta_\mathrm{i}/\mathrm{T})-1}\right] + \frac{3}{2}\mathrm{nRa_0x^mT^2}\frac{\mathrm{m}}{\mathrm{V}}. \tag{6}$$

Differentiating eq. (5) with respect to temperature at constant volume and eq. (6) with respect to volume at constant temperature, we obtain isochoric heat capacity and isothermal bulk modulus:

$$C_V = \left(\frac{\partial E_{th}}{\partial T}\right)_V = 3n\mathrm{R}\left[\left(\frac{\Theta_i}{T}\right)^2\frac{\exp(\Theta_i/T)}{[\exp(\Theta_i/T)-1]^2}\right] + 3n\mathrm{R}a_0x^mT, \tag{7}$$

$$K_{Tth} = -V\left(\frac{\partial P_{th}}{\partial V}\right)_T = 3n\mathrm{R}\left[\begin{array}{c}\frac{\gamma}{V}(1+\gamma-q)\left[\frac{\Theta_i}{\exp(\Theta_i/T)-1}\right] - \gamma^2\frac{T}{V}\left[\left(\frac{\Theta_i}{T}\right)^2\frac{\exp(\Theta_i/T)}{(\exp(\Theta_i/T)-1)^2}\right] + \\ +\frac{1}{2}a_0x^mT^2\frac{m}{V}(1-m)\end{array}\right] =$$

$$= P_{th}(1+\gamma-q) - \gamma^2 C_V\frac{T}{V} + \frac{3}{2}n\mathrm{R}a_0x^mT^2\frac{(mq-m\gamma-m^2+2\gamma^2)}{V}. \tag{8}$$

Differentiating eq. (6) with respect to temperature at constant volume, we determine slope:

$$(\partial P_{th}/\partial T)_V = 3n\mathrm{R}\frac{\gamma}{V}\left[\left(\frac{\Theta_i}{T}\right)^2\frac{\exp(\Theta_i/T)}{(\exp(\Theta_i/T)-1)^2}\right] + 3n\mathrm{R}a_0x^mT\frac{m}{V}. \tag{9}$$

The volume dependence of the characteristic temperatures in eq. (3), and unknown parameters γ and q in eq. (6, 8, 9) are taken from [*Al'tshuler et al., 1987*]:

$$\Theta_i = \Theta_{0i}x^{-\gamma_\infty}\exp\left[\frac{\gamma_0-\gamma_\infty}{\beta}(1-x^\beta)\right], \tag{10.1}$$

$$\gamma = -\left(\frac{\partial \ln\Theta_i}{\partial \ln V}\right)_T = \gamma_\infty + (\gamma_0-\gamma_\infty)x^\beta, \tag{10.2}$$

$$q = \left(\frac{\partial \ln\gamma}{\partial \ln V}\right)_T = \beta x^\beta\frac{\gamma_0-\gamma_\infty}{\gamma}, \tag{10.3}$$

where Θ_{0i} is characteristic temperature under standard conditions (i = 1, 2); γ_0 is the Grüneisen parameter under standard conditions; γ_∞ is the Grüneisen parameter at infinite compression, when $x \to 0$; β is an additional parameter.

To calculate the magnetic contribution to the Helmholtz free energy, we use the formalism from [*Dinsdale, 1991*], which was modified in [*Jacobs, Schmid-Fetzer, 2010*] to obtain the correct limit of the entropy at 0 K. The magnetic contribution is expressed as:

$$F_{mag}(T) = RT\ln(B_0 + 1)(g(\tau) - 1), \quad (11)$$

where B_0 is average magnetic moment per atom and $\tau = T/T_C$, T_C is Curie temperature.

The function $g(\tau)$ is obtained as:

$$g(\tau) = 1 - \left[\frac{79\tau^{-1}}{140p} + \frac{474}{497}\left(\frac{1}{p} - 1\right)\left(\frac{\tau^3}{6} + \frac{\tau^9}{135} + \frac{\tau^{15}}{600}\right)\right]/D, \text{ if } \tau \le 1, \quad (12.1)$$

$$g(\tau) = -\left(\frac{\tau^{-5}}{10} + \frac{\tau^{-15}}{315} + \frac{\tau^{-25}}{1500}\right)/D, \text{ if } \tau > 1. \quad (12.2)$$

The value D in eq. (12.1 and 12.2) is calculated as:

$$D = \frac{518}{1125} + \frac{11692}{15975}\left(\frac{1}{p} - 1\right), \quad (13)$$

where p is fraction of magnetic enthalpy.

The magnetic contribution in eq. (11) does not depend on pressure, so it will be equal for the Helmholtz free energy and Gibbs energy. The equations for the magnetic contribution to entropy, enthalpy and heat capacity are available in [*Dinsdale, 1991*]. The same formalism was used to construct the equation of state of bcc-Fe [*Dorogokupets et al., 2014*]. Eq. (11) is used to determine the magnetic contribution to one atom of chromium or iron. Therefore, the magnetic contribution in EoSes of eskolaite and hematite can be calculated with a multipler of 2, while the multiplier for magnetite is 3. Parameters B_0 and p in eq. (11, 13) for Cr_2O_3, α-Fe_2O_3, and Fe_3O_4 are determined by fitting the heat capacity in the region λ-anomaly.

The total pressure and isothermal bulk modulus are calculated as the sums of potential and thermal parts: $P=P_0(V)+P_{th}(V,T)$, $K_T=K_{T0}(V)+K_{Tth}(V,T)$, respectively. Then we can calculate the volume coefficient of thermal expansivity $\alpha=(\partial P_{th}/\partial T)_V/K_T$, heat capacity at constant pressure $C_P=C_V+\alpha^2TVK_T$, adiabatic bulk modulus $K_S=K_T+VT(\alpha K_T)^2/C_V$, and thermodynamic Grüneisen parameter $\gamma_{th}=\alpha VK_T/C_V=\alpha VK_S/C_P$. Enthalpy and the Gibbs energy are determined from the linear relationships: $H=E+PV$, $G=F(V, T)+PV$, respectively.

Adding up the corresponding functions, we obtain a complete thermodynamic description of equation of state. Equations (1–13) contain fixed parameters U_0, V_0, K_0, K', m_1, m_2, R, T_C, and the group of fitted parameters Θ_{01}, Θ_{02}, γ_0, γ_∞, β, a_0, m, B_0, and p, which are derived by the least squares method. Table 1 shows the EoSes parameters of rock-forming oxides (α-Al_2O_3, Cr_2O_3, α-Fe_2O_3, and Fe_3O_4), which are obtained by simultaneous optimization of experimental measurements of heat capacity, molar volume, thermal expansion, adiabatic bulk modulus at ambient pressure, and *P-V-T* measurements at the reference isotherm and at high temperatures.

Table 1. **Parameters of equations of state of rock-forming oxides**

Таблица 1. **Параметры уравнений состояния породообразующих оксидов**

Parameters	α-Al_2O_3	Cr_2O_3	α-Fe_2O_3	Fe_3O_4
U_0, kJmol^{-1}	–1690.49	–1161.25	–851.78	–1158.10
V_0, cm^{3}mol^{-1}	25.575	29.057	30.274	44.580
K_0, GPa	252.3	211.7	202.5	181.2
K'	4.14	5.35	3.21	4.90
Θ_{10}, K	956	718	554	613
m_1	7.5	7.5	11.9	10.5
Θ_{20}, K	475	376	201	252
m_2	7.5	7.5	3.1	10.5
γ_0	1.323	1.388	2.084	1.341
B	1.725	0.5	1.3	0.9
a_0, 10^{-6}K^{-1}	8.2	–	–	43.7
m	1.0	–	–	1.0
T_C, K	–	307	950	845.5
B_0	–	1.034	1.927	3.751
p	–	0.378	0.304	0.321

3. Equation of state of α-Al_2O_3

The equation of state of corundum is constructed according to the thermodynamic model using eq. (1–10). Figures 1–3 show the calculated thermodynamic functions of corundum depending on temperature at 1 bar pressure in comparison with various experimental measurements. The calculated heat capacity of α-Al_2O_3 (Fig. 1) is in good agreement with measurements from [*Goto et al., 1989; Archer, 1993*] and reference data from [*Gurvich et al., 1981; Chase, 1998*]. The calculated coefficient of volumetric thermal expansivity (Fig. 2) is in close agreement with measurements from [*Wachtman et al., 1962; Schauer, 1965; Kirby et al., 1972; White, Roberts, 1983*], but slightly differs from the measurements from [*Aldebert, Traverse, 1984; Goto et al., 1989; Saxena, Shen, 1992*] at temperatures above 1200 K. The calculated adiabatic and isothermal bulk modulus (Fig. 3) is consistent with the data from [*Chung, Simmons, 1968; Goto et al., 1989; Anderson, Isaak, 1995*].

The calculated parameters of the reference isotherm of corundum are based on the quasi-hydrostatic measurements in a helium pressure-transmitting medium from [*Dewaele, Torrent, 2013*]. Pressure is measured using the ruby scale from [*Dorogokupets, Oganov, 2007*], which slightly underestimates pressure compared to the new calibration of the ruby pressure scale in [*Dorogokupets et al., 2012; Sokolova et al., 2013*]. The parameters of the equation of state of corundum according [*Dewaele, Torrent, 2013*] are as follows: V_0=25.64 cm^{3}mol^{-1}, K_0=254.1 GPa, and K'=4.00 (Rydberg-Vinet equation, the ruby scale from [*Dorogokupets, Oganov, 2007*]). All the experimental *P-V-T* measurements are given in the form of $x=V/V_0$, where V_0 is the proposed reference value. Experimental data from [*Dewaele, Torrent, 2013*] are calculated based on the ruby pressure scale from [*Sokolova et al., 2013*] and using V_0=25.575 cm^{3}mol^{-1} from [*Robie et al., 1978*]. We have obtained for corundum: K_0=252.3 GPa, K'=4.14, and these values are in good agreement with the ultrasonic measurements reported in [*Chung, Simmons, 1968; Goto et al., 1989; Anderson, Isaak, 1995*]. Figure 4 shows that the calculated reference isotherm of corundum is consistent with the recalculated data from [*Dewaele, Torrent, 2013*], but earlier measurements [*Richet et al., 1988; Dubrovinsky et al., 1998; Jephcoat et al., 1988; Funamori, Jeanloz, 1997*] give a higher pressure. It should be noted that our calculations are in good agreement with the first studies of corundum compressibility [*d'Amur et al., 1978; Finger, Hazen, 1978*] in the classic hydrostatic conditions (4:1 volume mixture of methanol-ethanol). Figure 5 shows the deviation of the high-temperature measurements of compressibility [*Dubrovinsky et al., 1998; Grevel et al., 2000*] from our calculations. In [*Grevel et al., 2000*], pressure was calculated using NaCl pressure marker from [*Decker, 1971*]. According to [*Strässle et al., 2014*], this scale underestimates pressure up to 0.5 GPa (at 10–15 GPa) in comparison with NaCl EoS from [*Brown, 1999*]. Values more consistent with our EoS calculations for corundum can be obtained by recalculating the data from [*Grevel et al., 2000*] using NaCl scale from [*Brown, 1999*]. The data from [*Dubrovinsky et al., 1998*] significantly overstate the pressure probably due to the pressure measurement method.

The calculated thermodynamic functions of α-Al_2O_3 depending on temperature at pressures 0.0001, 50, and 80 GPa are presented in Table 2. The last two columns show the increments of the Gibbs energy of corundum at given temperatures and pressures, which are calculated from our data and database in [*Holland, Powell, 2011*] (G and G^*, respectively). The Gibbs energy under standard conditions is calculated with regard to ΔH_{298}=–1675.33 kJmol^{-1} [*Holland, Powell, 2011*] and standard entropy S_{298}=50.841 Jmol^{-1}K^{-1} (Table 2) as follows: $G_{298}=\Delta H_{298}-S_{298}*298.15$. In our equation of state, the Gibbs energy under standard conditions is defined by parameter U_0, therefore $G_{298}=U_0$=–1690.49 kJmol^{-1}. The calculated *P-V-T* relations of corundum can be used for pressure calculations at given temperatures and volumes, which is important for practical aspects of the high-pressure experiments.

4. Equations of state of Cr_2O_3, α-Fe_2O_3, and Fe_3O_4

The magnetic contribution to the Helmholtz free energy is considered in the equations of state of eskolaite, hematite and magnetite using eq. (1–13). A specific λ-type anomaly in the heat capacity of minerals is indicative of the magnetic transition of atoms or rare structural changes as shown for α-SiO_2 → coesite transformation [*Dorogokupets, 1995*]. Curie point (T_C) determines the critical state that marks a sharp change in the magnetic properties of minerals.

Figures 6–8 show the calculated heat capacities of Cr_2O_3, α-Fe_2O_3, and Fe_3O_4 in comparison with the experimental measurements. The shape of the λ-type anomaly in the heat capacity of oxides is well described by the EoS suggested in this study. The calculated heat capacity of Cr_2O_3 is in good agreement with measurements reported in [*Bruce, Cannel, 1977; Klemme et al., 2000; Ziemniak et al., 2007; Gurevich et al., 2009; Aristova, Gusarov, 2008*]. The heat capacities of α-Fe_2O_3 and Fe_3O_4 are consistent with the data from the experiments described in [*Gronvold, Westrum, 1959; Westrum, Gronvold, 1969; Gronvold, Sveen, 1974; Gronvold, Samuelsen, 1975; Hemingway, 1990; Shebanova, Lazor, 2003; Snow et al., 2010*] and the reference data [*Robie et al., 1978*]. Cr_2O_3 undergoes antiferromagnetic–paramagnetic transition at T_C=307 K. The temperature of this magnetic transition is close to 300 K,

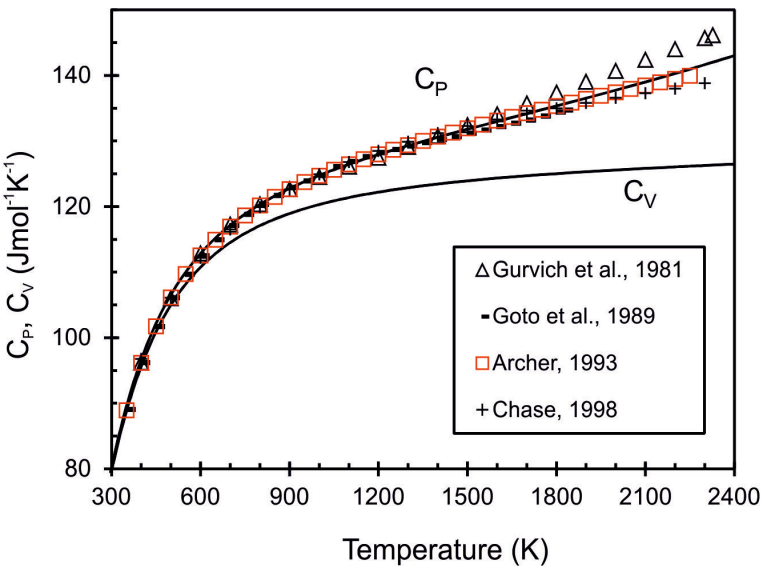

Fig. 1. Calculated isobaric (C_P) and isochoric (C_V) heat capacity of α-Al_2O_3 (solid lines) in comparison with selected reference and experimental data [*Gurvich et al., 1981; Goto et al., 1989; Archer, 1993; Chase, 1998*].

Рис. 1. Рассчитанная изобарная (C_P) и изохорная (C_V) теплоемкость α-Al_2O_3 (линии) в сравнении со справочными и экспериментальными данными [*Gurvich et al., 1981; Goto et al., 1989; Archer, 1993; Chase, 1998*].

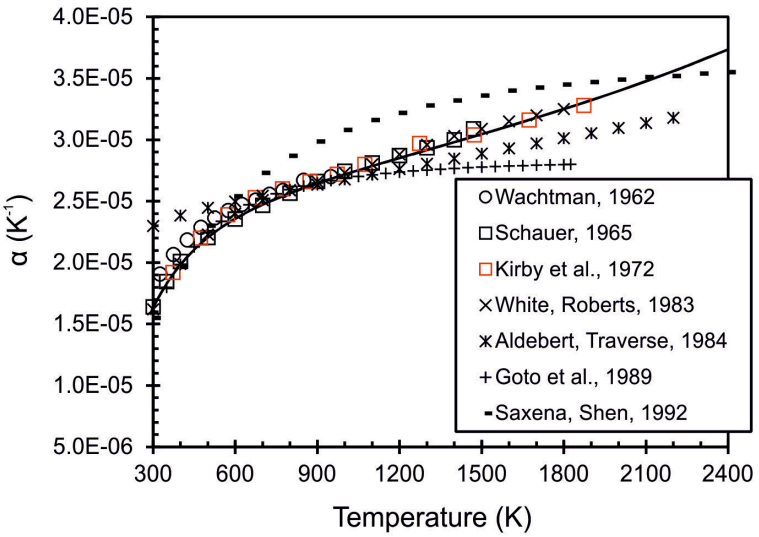

Fig. 2. Calculated coefficient of volumetric thermal expansion of α-Al_2O_3 (solid line) in comparison with selected reference and experimental data [*Wachtman et al., 1962; Schauer, 1965; Kirby et al., 1972; White, Roberts, 1983; Aldebert, Traverse, 1984; Goto et al., 1989; Saxena, Shen, 1992*].

Рис. 2. Рассчитанный коэффициент термического расширения α-Al_2O_3 (линия) в сравнении со справочными и экспериментальными данными [*Wachtman et al., 1962; Schauer, 1965; Kirby et al., 1972; White, Roberts, 1983; Aldebert, Traverse, 1984; Goto et al., 1989; Saxena, Shen, 1992*].

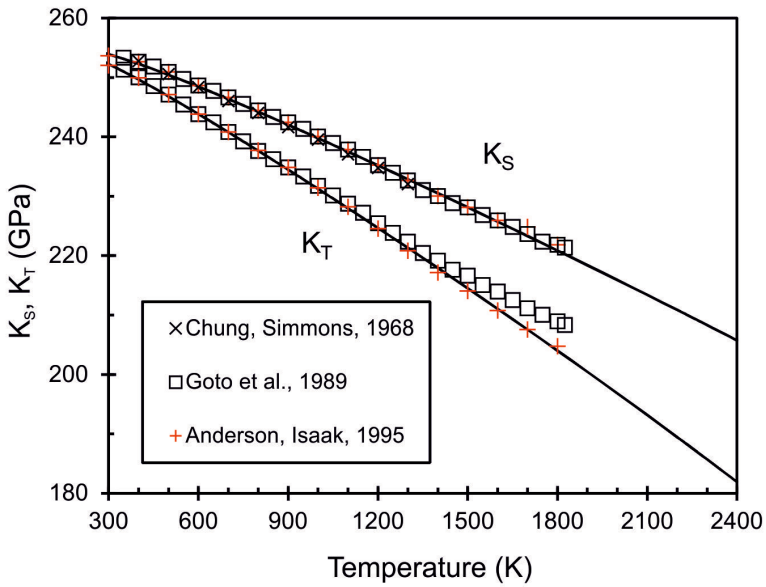

Fig. 3. Calculated isothermal (K_T) and adiabatic (K_S) bulk moduli of α-Al_2O_3 in comparison with experimental data [*Chung, Simmons, 1968; Goto et al., 1989; Anderson, Isaak, 1995*].

Рис. 3. Рассчитанные изотермический (K_T) и адиабатический (K_S) модули сжатия α-Al_2O_3 в сравнении с экспериментальными данными [*Chung, Simmons, 1968; Goto et al., 1989; Anderson, Isaak, 1995*].

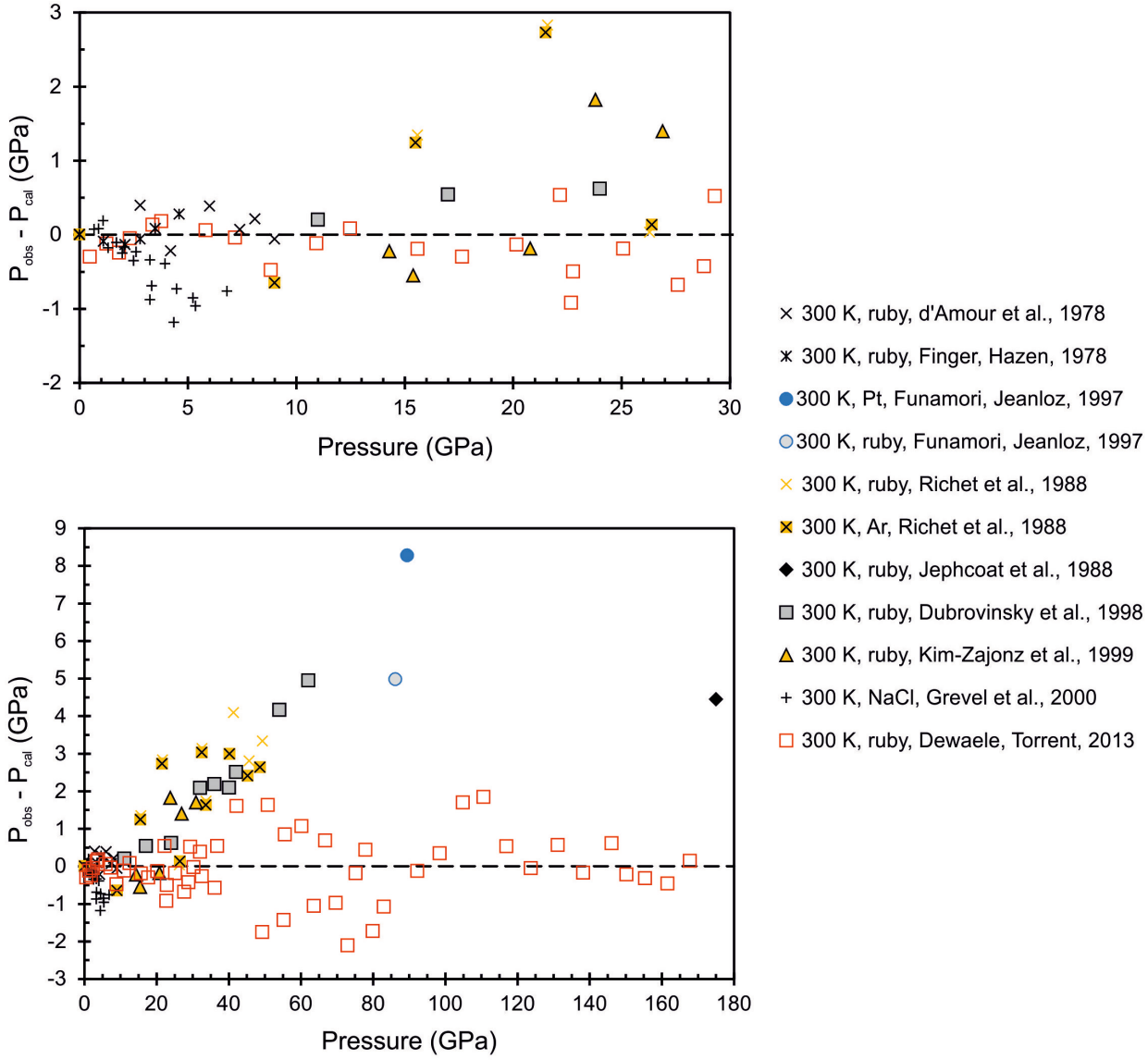

Fig. 4. Difference between observed pressure (P_{obs}) [*Dewaele, Torrent, 2013; Richet et al., 1988; Kim-Zajonz et al., 1999; Grevel et al., 2000; Dubrovinsky et al., 1998; Jephcoat et al., 1988; Funamori, Jeanloz, 1997; d'Amour et al., 1978; Finger, Hazen, 1978*] and calculated pressure (P_{cal}) from equation of state of corundum at 300 K isotherm. The measurements in [*Dewaele, Torrent, 2013*] are recalculated to the ruby scale from [*Dorogokupets et al., 2012; Sokolova et al., 2013*]. The upper figure is limited to a pressure 30 GPa.

Рис. 4. Разница между измеренным давлением (P_{obs}) [*Dewaele, Torrent, 2013; Richet et al., 1988; Kim-Zajonz et al., 1999; Grevel et al., 2000; Dubrovinsky et al., 1998; Jephcoat et al., 1988; Funamori, Jeanloz, 1997; d'Amour et al., 1978; Finger, Hazen, 1978*] и рассчитанным давлением (P_{cal}) по уравнению состояния корунда на изотерме 300 К. Измерения из работы [*Dewaele, Torrent, 2013*] были пересчитаны на основе рубиновой шкалы из работ [*Dorogokupets et al., 2012; Sokolova et al., 2013*]. Верхний рисунок приведен для области низких давлений до 30 ГПа.

making it difficult to precisely measure. Magnetic transitions for α-Fe_2O_3 and Fe_3O_4 are calculated at 950 K and 845.5 K, respectively.

The deviations in the pressures calculated from the EoS of eskolaite in this study and observed in [*Dymshits et al., 2016*] are limited to $\Delta P/P$=±1.5 % up to 1873 K (Fig. 9). The difference between pressures does to exceed ±1 GPa in the measurements at reference isotherm [*Sato, Akimoto, 1979; Finger, Hazen, 1980; Kantor et al., 2012*]. The difference between the observed pressure and calculated pressure from equations of state of hematite and magnetite at the reference isotherm is $\Delta P/P$=±0.6 % (Fig. 10 *a, b*). Thus, the proposed equations of state of Cr_2O_3, α-Fe_2O_3, and Fe_3O_4 are in good agreement with the experimental studies of these minerals.

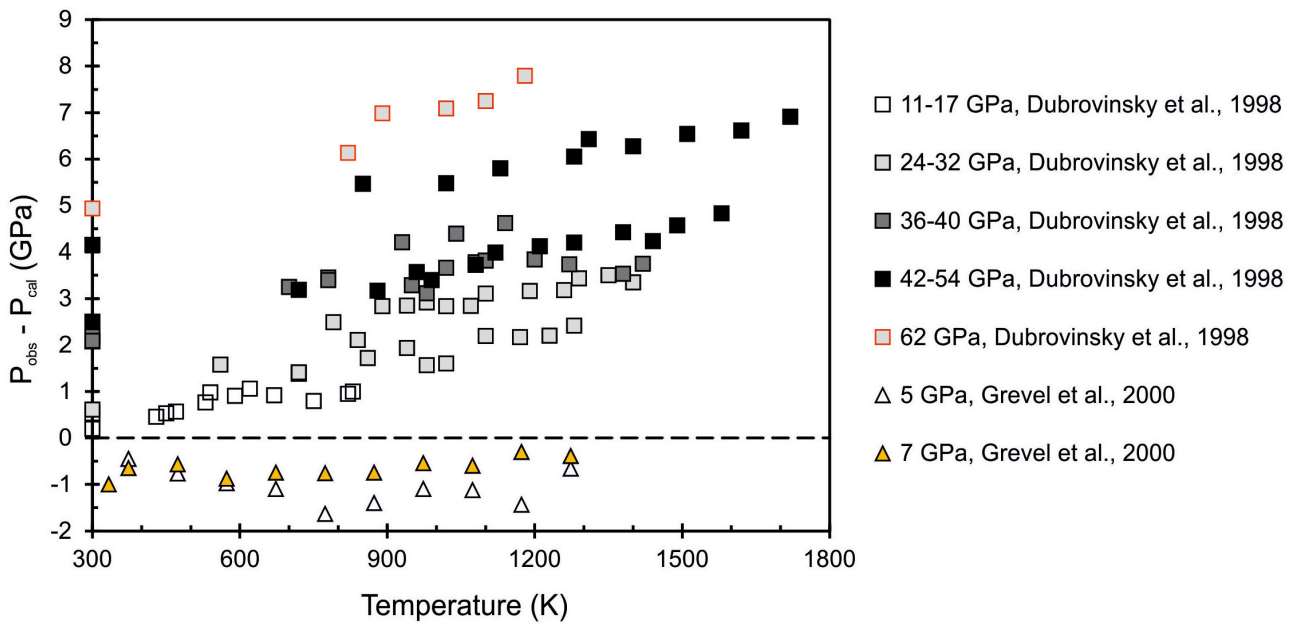

Fig. 5. Difference between observed pressure (P_{obs}) [*Dubrovinsky et al., 1998; Grevel et al., 2000*] and calculated pressure (P_{cal}) from equation of state of corundum at high temperatures.

Рис. 5. Разница между измеренным давлением (P_{obs}) [*Dubrovinsky et al., 1998; Grevel et al., 2000*] и рассчитанным давлением (P_{cal}) по уравнению состояния корунда при высоких температурах.

The calculated thermodynamic functions of Cr_2O_3, α-Fe_2O_3, and Fe_3O_4 depending on temperature at different pressures are listed in Tables 3–5. The calculated Gibbs energy under standard conditions for Cr_2O_3 ($G_{298}=U_0=-1161.25$ kJmol^{-1}), α-Fe_2O_3 ($G_{298}=U_0=-851.78$ kJmol^{-1}) and Fe_3O_4 ($G_{298}=U_0=-1158.10$ kJmol^{-1}) agree well with the results reported in [*Holland, Powell, 2011*] (G^* in Tables 3–5).

T a b l e 2. **Thermodynamic functions of α-Al_2O_3 calculated at different pressures**

T а б л и ц а 2. **Рассчитанные термодинамические функции α-Al_2O_3 при разных давлениях**

P	T	$x=V/V_0$	α	S	C_P	C_V	K_T	K_S	γ_{th}	G	G^*
GPa	K		10^{-6}K^{-1}		Jmol^{-1}K^{-1}		GPa			kJmol^{-1}	
0.0001	298.15	1.00000	16.223	50.841	79.702	79.196	252.30	253.91	1.32	–1690.49	–1690.43
0.0001	500	1.00396	22.034	99.557	106.494	104.956	246.82	250.44	1.33	–1705.86	–1705.85
0.0001	1000	1.01659	27.170	180.516	124.729	120.290	231.24	239.77	1.36	–1777.69	–1777.66
0.0001	1500	1.03135	30.449	232.521	131.778	123.910	214.50	228.13	1.39	–1881.70	–1881.54
0.0001	2000	1.04807	33.969	271.243	137.736	125.561	196.82	215.90	1.43	–2008.04	–2007.76
50	298.15	0.86330	7.179	38.199	68.078	67.928	439.98	440.94	1.03	–509.29	–507.54
50	500	0.86488	10.458	81.777	98.481	97.953	436.06	438.40	1.03	–521.51	–519.25
50	1000	0.87009	12.976	158.419	119.401	117.811	424.46	430.19	1.04	–583.17	–580.00
50	1500	0.87599	13.967	208.100	125.240	122.538	412.08	421.16	1.05	–675.54	–671.10
50	2000	0.88230	14.721	244.597	128.450	124.545	399.30	411.83	1.07	–789.12	–784.89
80	298.15	0.81198	5.245	34.264	63.917	63.824	541.42	542.20	0.92	132.51	136.95
80	500	0.81308	7.878	75.950	95.500	95.153	537.97	539.94	0.93	121.30	126.61
80	1000	0.81680	9.894	151.108	117.861	116.782	527.56	532.43	0.93	63.01	69.89
80	1500	0.82101	10.598	200.205	123.809	121.982	516.39	524.13	0.94	–25.55	–17.46
80	2000	0.82548	11.076	236.262	126.766	124.151	504.90	515.54	0.95	–135.06	–126.12

N o t e. G – data calculated in this study; G^* – data from [*Holland, Powell, 2011*].

П р и м е ч а н и е. G – данные, рассчитанные в настоящей работе; G^* – данные из работы [*Holland, Powell, 2011*].

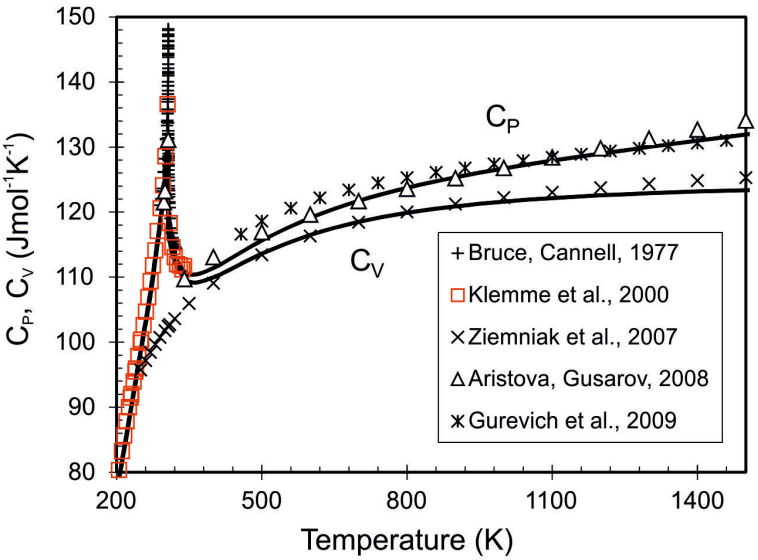

Fig. 6. Calculated isobaric and isochoric heat capacity of Cr_2O_3 (solid lines) in comparison with selected reference and experimental data [*Bruce, Cannel, 1977; Klemme et al., 2000; Ziemniak et al., 2007; Aristova, Gusarov, 2008; Gurevich et al., 2009*].

Рис. 6. Рассчитанная изобарная и изохорная теплоемкость Cr_2O_3 (линии) в сравнении со справочными и экспериментальными данными [*Bruce, Cannel, 1977; Klemme et al., 2000; Ziemniak et al., 2007; Aristova, Gusarov, 2008; Gurevich et al., 2009*].

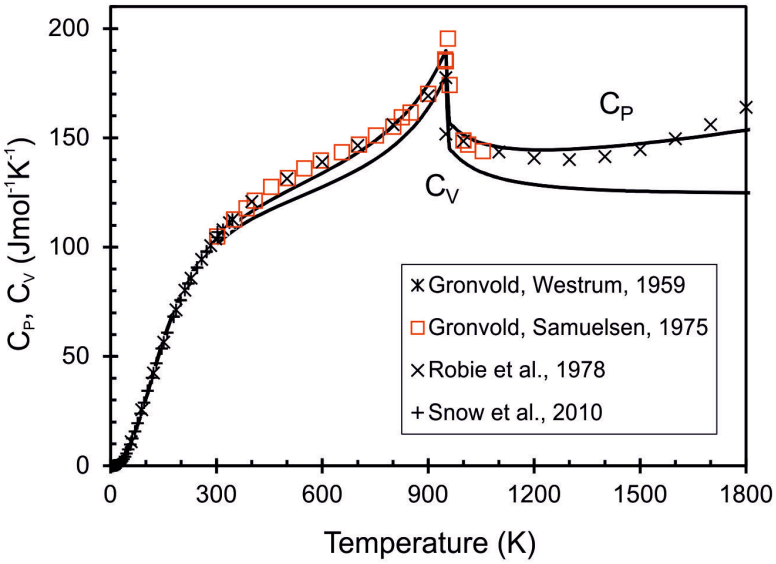

Fig. 7. Calculated isobaric and isochoric heat capacity of α-Fe_2O_3 (solid lines) in comparison with selected reference and experimental data [*Gronvold, Westrum, 1959; Gronvold, Samuelsen, 1975; Robie et al., 1978; Snow et al., 2010*].

Рис. 7. Рассчитанная изобарная и изохорная теплоемкость α-Fe_2O_3 (линии) в сравнении со справочными и экспериментальными данными [*Gronvold, Westrum, 1959; Gronvold, Samuelsen, 1975; Robie et al., 1978; Snow et al., 2010*].

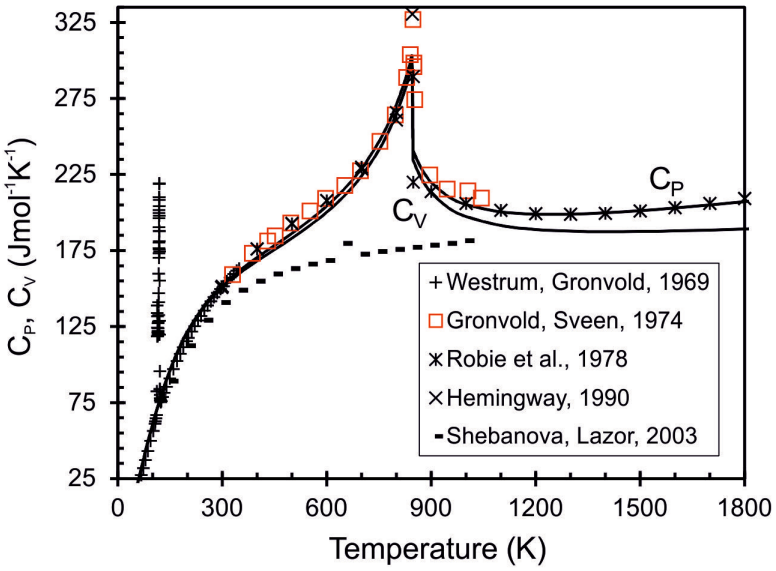

Fig. 8. Calculated isobaric and isochoric heat capacity of Fe_3O_4 (solid lines) in comparison with selected reference and experimental data [*Westrum, Gronvold, 1969; Gronvold, Sveen, 1974; Robie et al., 1987; Hemingway, 1990; Shebanova, Lazor, 2003*].

Рис. 8. Рассчитанная изобарная и изохорная теплоемкость Fe_3O_4 (линии) в сравнении со справочными и экспериментальными данными [*Westrum, Gronvold, 1969; Gronvold, Sveen, 1974; Robie et al., 1978; Hemingway, 1990; Shebanova, Lazor, 2003*].

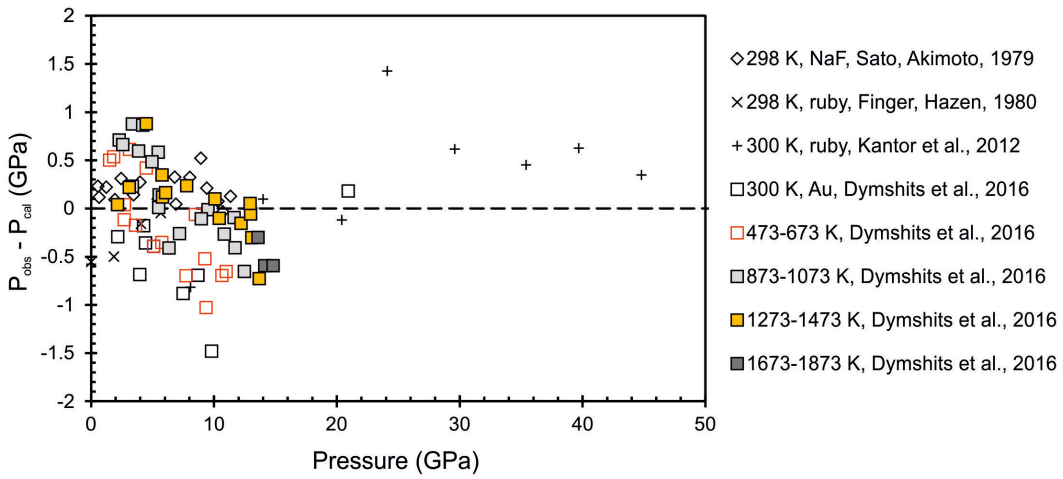

Fig. 9. Difference between observed pressure in [*Sato, Akimoto, 1979; Finger, Hazen, 1980; Kantor et al., 2012; Dymshits et al., 2016*] and calculated pressure from equation of state of eskolaite at the isotherms 298 to 1873 K.

Рис. 9. Разница между измеренным давлением в работах [*Sato, Akimoto, 1979; Finger, Hazen, 1980; Kantor et al., 2012; Dymshits et al., 2016*] и рассчитанным давлением по уравнению состояния эсколаита на изотермах от 298 до 1873 К.

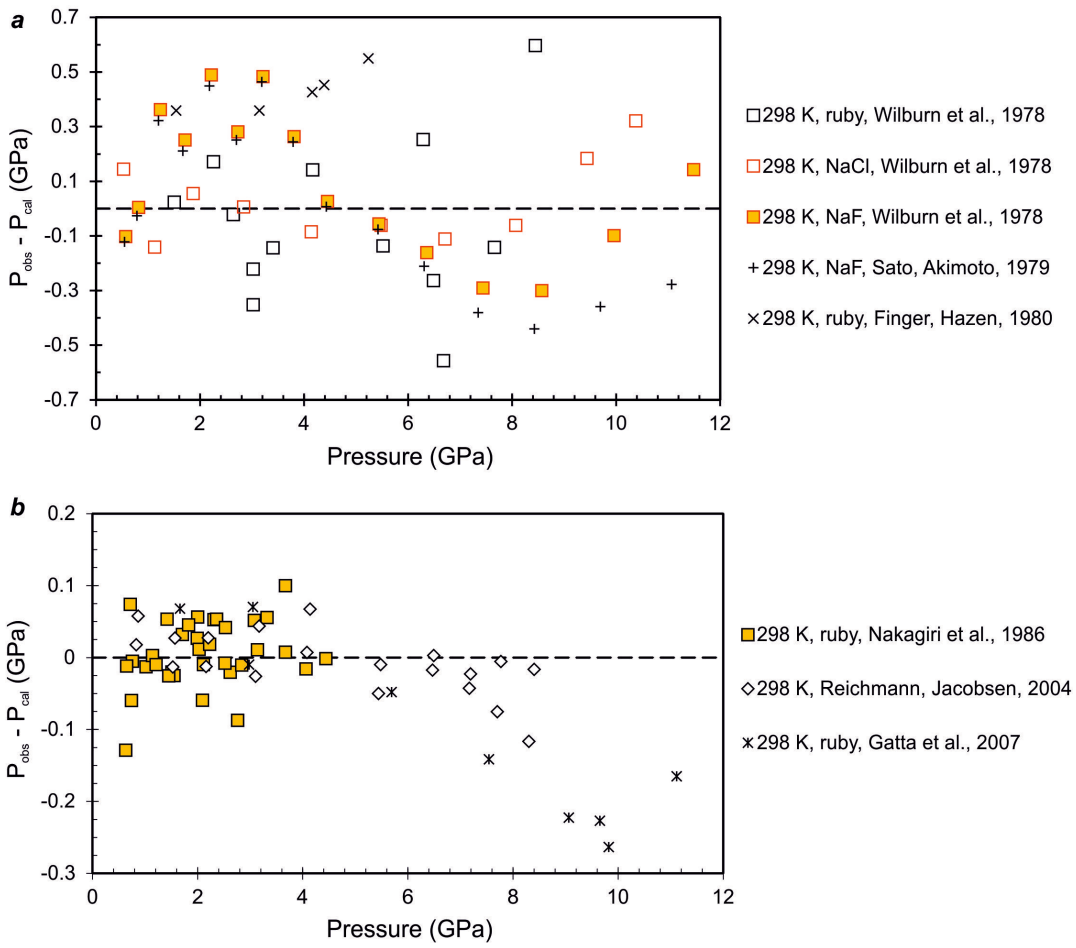

Fig. 10. Difference between observed pressure in [*Wilburn et al., 1978; Sato, Akimoto, 1979; Finger, Hazen, 1980; Nakagiri et al., 1986; Reichmann, Jacobsen, 2004; Gatta et al., 2007*] and calculated pressure from equation of state of hematite (*a*) and magnetite (*b*) at the reference isotherm 298 K.

Рис. 10. Разница между измеренным давлением в работах [*Wilburn et al., 1978; Sato, Akimoto, 1979; Finger, Hazen, 1980; Nakagiri et al., 1986; Reichmann, Jacobsen, 2004; Gatta et al., 2007*] и рассчитанным по уравнениям состояния гематита (*a*) и магнетита (*b*) на отсчетной изотерме 298 К.

Table 3. **Thermodynamic functions of Cr_2O_3 calculated at different pressures**

Таблица 3. **Рассчитанные термодинамические функции Cr_2O_3 при разных давлениях**

P	*T*	*x=V/V₀*	*α*	*S*	*C_P*	*C_V*	*K_T*	*K_S*	γth	*G*	*G**
GPa	K		$10^{-6}K^{-1}$		$Jmol^{-1}K^{-1}$		GPa			$kJmol^{-1}$	
0.0001	298.15	1	21.211	80.2160	123.793	122.968	211.70	213.12	1.06	−1161.25	−1162.08
0.0001	500	1.0049	25.942	138.785	115.587	113.560	206.32	210.00	1.38	−1183.87	−1185.12
0.0001	1000	1.0191	29.951	223.073	126.685	121.584	192.02	200.08	1.40	−1276.44	−1279.12
0.0001	1500	1.0352	32.669	275.479	131.894	123.358	177.27	189.53	1.41	−1401.87	−1406.11
0.0001	2000	1.0530	35.586	314.057	136.553	123.984	162.18	178.62	1.42	−1549.66	−1555.56
30	298.15	0.8986	12.133	67.1730	115.728	115.317	358.64	359.92	0.99	−338.36	−335.46
30	500	0.9012	15.427	122.491	110.858	109.755	353.95	357.51	1.30	−357.97	−356.14
30	1000	0.9088	17.672	204.185	123.270	120.454	341.43	349.41	1.32	−441.63	−443.61
30	1500	0.9171	18.642	255.037	127.392	122.827	328.63	340.84	1.33	−557.22	−563.66
30	2000	0.9259	19.446	292.070	130.097	123.673	315.72	332.12	1.34	−694.41	−705.81
70	298.15	0.8207	7.8670	57.5000	108.557	108.323	531.94	533.09	0.92	657.16	663.17
70	500	0.8223	10.459	109.899	106.693	106.004	527.65	531.08	1.24	639.85	644.49
70	1000	0.8270	12.141	189.579	121.136	119.308	516.02	523.93	1.26	563.11	562.46
70	1500	0.8322	12.702	239.588	125.241	122.291	504.14	516.30	1.27	455.04	448.14
70	2000	0.8376	13.083	275.943	127.464	123.364	492.18	508.53	1.27	325.75	311.88

5. Discussion and conclusion

In this study, the equations of state of rock-forming oxides (α-Al_2O_3, Cr_2O_3, α-Fe_2O_3, and Fe_3O_4) are developed based on optimization of variety experimental measurements and can be used for calculation of different thermodynamic properties in a wide range of pressures and temperatures. The proposed approach for constructing of equation of state perfectly approximates the thermochemical data of the heat capacity and allows one to describe the λ-type anomaly in case of changes in magnetic properties of Cr_2O_3, α-Fe_2O_3, and Fe_3O_4.

Nonetheless, other studies concerning equations of state (especially for corundum) are noteworthy. In [*Dubrovinskaya et al., 1997*], the equation of state is based on the Helmholtz free energy with a single set of common parameters and the Birch-Murnaghan equation on zero isotherm. In this study, the extrapolations of the heat capacity, thermal expansion, elastic moduli and *P-V-T* properties to high pressures and temperatures are in good agreement with the experimental data. In the computational study reported in [*Dorogokupets et al., 1999*], an empirical model is constructed for the joint optimization of data on isobaric heat capacity, volume, thermal expansion coefficient, and

Table 4. **Thermodynamic functions of α-Fe_2O_3 calculated at different pressures**

Таблица 4. **Рассчитанные термодинамические функции α-Fe_2O_3 при разных давлениях**

P	*T*	*x=V/V₀*	*α*	*S*	*C_P*	*C_V*	*K_T*	*K_S*	γth	*G*	*G**
GPa	K		$10^{-6}K^{-1}$		$Jmol^{-1}K^{-1}$		GPa			$kJmol^{-1}$	
0.0001	298.15	1	33.873	87.695	102.870	100.773	202.50	206.71	2.06	−851.78	−851.65
0.0001	500	1.0076	40.449	146.916	125.411	120.511	196.37	204.35	2.01	−875.78	−875.81
0.0001	1000	1.0301	46.982	248.732	151.340	138.892	180.85	197.05	1.91	−975.50	−977.81
0.0001	1500	1.0560	52.498	307.882	147.287	125.514	164.74	193.32	2.20	−1116.21	−1119.53
0.0001	2000	1.0858	59.146	351.684	158.678	124.668	147.88	188.22	2.31	−1281.57	−1285.98
20	298.15	0.9175	23.348	71.4180	93.8630	92.673	263.70	267.09	1.85	−272.74	−270.04
20	500	0.9224	29.062	126.977	119.836	116.791	258.25	264.98	1.79	−293.02	−291.12
20	1000	0.9372	33.595	225.228	145.669	137.842	244.42	258.30	1.69	−381.78	−384.52
20	1500	0.9537	36.394	281.513	138.242	125.032	230.30	254.63	1.94	−510.03	−516.75
20	2000	0.9719	39.250	321.999	143.954	124.391	215.79	249.73	2.00	−661.41	−672.81
50	298.15	0.8314	15.352	56.4180	83.2700	82.6550	347.78	350.36	1.63	518.99	534.37
50	500	0.8344	20.335	107.672	113.547	111.755	342.98	348.48	1.58	502.25	516.41
50	1000	0.8439	23.846	202.484	141.166	136.363	330.66	342.31	1.48	424.15	431.64
50	1500	0.8544	25.431	256.725	132.330	124.347	318.15	338.57	1.68	307.79	308.70
50	2000	0.8656	26.790	295.184	135.486	123.997	305.43	333.73	1.73	169.30	162.50

T a b l e 5. **Thermodynamic functions of Fe_3O_4 calculated at different pressures**

T а б л и ц а 5. **Рассчитанные термодинамические функции Fe_3O_4 при разных давлениях**

P	*T*	*x=V/V₀*	*α*	*S*	*C_P*	*C_V*	*K_T*	*K_S*	γ_{th}	*G*	*G**
GPa	K		$10^{-6}K^{-1}$		$Jmol^{-1}K^{-1}$		GPa			$kJmol^{-1}$	
0.0001	298.15	1	24.251	146.246	151.503	150.087	181.20	182.91	1.31	–1158.10	–1158.27
0.0001	500	1.0054	28.235	233.239	186.151	183.001	176.33	179.37	1.22	–1196.85	–1197.39
0.0001	1000	1.0209	32.553	387.280	205.181	197.300	163.43	169.96	1.23	–1355.10	–1357.68
0.0001	1500	1.0386	36.341	468.424	201.166	187.424	149.83	160.82	1.35	–1570.44	–1575.12
0.0001	2000	1.0588	40.832	527.662	211.941	190.604	135.56	150.74	1.37	–1820.04	–1827.81
10	298.15	0.9522	18.916	136.960	147.615	146.581	228.34	229.95	1.25	–723.45	–724.10
10	500	0.9562	22.177	222.341	183.605	181.259	223.82	226.72	1.17	–760.15	–760.04
10	1000	0.9677	25.214	374.643	202.257	196.446	211.88	218.15	1.17	–912.48	–911.40
10	1500	0.9805	27.470	454.289	196.413	186.547	199.41	209.95	1.28	–1121.13	–1118.73
10	2000	0.9947	29.893	511.790	204.276	189.499	186.46	201.00	1.30	–1363.24	–1359.93
20	298.15	0.9149	15.603	129.825	144.433	143.626	272.65	274.18	1.21	–307.59	–308.91
20	500	0.9181	18.440	213.912	181.640	179.772	268.38	271.16	1.13	–342.69	–342.29
20	1000	0.9272	20.849	364.985	200.368	195.749	257.06	263.13	1.13	–490.46	–486.60
20	1500	0.9373	22.435	443.709	193.608	185.870	245.28	255.49	1.24	–694.05	–686.11
20	2000	0.9482	24.036	500.223	200.070	188.684	233.12	247.19	1.26	–930.63	–918.69

bulk moduli of minerals at room pressure. The internal energy and isochoric heat capacity in this study are approximated by the Nernst-Lindeman function. The comparison of the Nernst-Lindeman function and our model with two characteristic temperatures (eq. 3) shows that the approximations look almost identical, so in both cases they provide good smoothing and approximation of the heat capacity, thermal expansion coefficient, and bulk moduli at reference pressure. Besides, other EoSes are available to calculate thermodynamic properties of corundum at high temperatures and pressures, such as described in [*Jacobs, Oonk, 2001; Jacobs, Shmid-Fetzer, 2010; Jacobs et al., 2013; Stixrude, Lithgow-Bertelloni, 2005; Brosh et al., 2008; Otero-de-la-Roza, Luana, 2011*].

The formalism in studies by *Gerya et al.* [*1998, 2004*] is considered thermodynamics of minerals based on the Gibbs energy. It is of special interest and may be used to construct the equations of state of corundum and phases with λ-type anomaly in the heat capacity, including Cr_2O_3, α-Fe_2O_3, and Fe_3O_4.

The thermodynamic properties of rock-forming oxides, which are established in this study, can provide a very useful contribution for geobarometry and modeling of the mineral composition of the Earth. The presence of sesquioxide stabilizes in the solid-state systems at depth and plays an important role in understanding the mantle mineralogy and structural transformations, which associated with the global and intermediate boundaries in the Earth's mantle (olivine → wadsleyite → ringwoodite; kyanite → corundum + stishovite; garnet → perovskite + corundum–ilmenite) [*Pushcharovsky, Pushcharovsky, 2010*]. Modeling of solid solutions based on iron oxide can be highly important for describing possible associations in the Earth's core and its solubility in the mantle phases. Chromium oxide with small concentrations of iron and aluminum was discovered as inclusions in diamond from the Udachnaya kimberlite pipe, Yakutia [*Logvinova et al., 2008*]. Because correct thermal equation of state of this phase is lacking it is impossible to calculate the released pressure of such inclusions.

The rock-forming oxides may form solid solutions with spinel structure. These spinel phases may contain variable amounts of trivalent cations Fe^{3+}, Al^{3+} and Cr^{3+} and divalent cations Fe^{2+} and Mg^{2+}. The properties of such materials are interesting and important for not only geology and geophysics. The refractoriness of some of these oxides is recognized as an extremely valuable characteristic in certain special applications in steelmaking furnace industry. Therefore, the temperature dependence of elastic and thermodynamic parameters, such as cell volume, bulk modulus, thermal expansion and the Grüneisen parameter of oxides, are significant for understanding the material dynamics with respect to thermal and pressure stress. The phase relations of the Cr_2O_3–Fe_2O_3–Al_2O_3 system at reference pressure have been known for more than 50 years [*Muan, Somiya, 1959; Schultz, Stubican, 1970*], but the knowledge of high-pressure behavior is still lacking.

The thermodynamic parameters of corundum, eskolaite, hematite, and magnetite, which are calculated in this study, specify the thermodynamics of pure oxide phases according to the current *P-V-T* measurements obtained in diamond anvils and multianvil apparatus [*Dewaele, Torrent, 2013; Dymshits et al., 2016*], and can be applied in calculations of more complex mineral systems and solid solutions at high temperatures and pressures.

6. Acknowledgments

We thanks PhD B.S. Danilov for his help in calculations of the Gibbs energy from the database [*Holland, Powell, 2011*]. This study was supported by the Russian Scientific Foundation (Project no 14-17-00601) and the Russian Foundation of Basic Research (Projects no. 15-35-20556 and 16-35-00061) and conducted under the program of the Ministry of Education and Science of the Russian Federation (Project no 14.B.25.31.0032).

7. Литература / References

Aldebert P., Traverse J.P., 1984. α-Al_2O_3: A high temperature thermal expansion standard. *High Temperatures. High Pressures* 16 (2), 127–135.

Al'tshuler L.V., Brusnikin S.E., Kuz'menkov E.A., 1987. Isotherms and Grüneisen functions for 25 metals. *Journal of Applied Mechanics and Technical Physics* 28 (1), 129–141. http://dx.doi.org/10.1007/BF00918785.

d'Amour H., Schiferl D., Denner W., Schulz H., Holzapfel W.B., 1978. High-pressure single-crystal structure determinations for ruby up to 90 kbar using an automatic diffractometer. *Journal of Applied Physics* 49 (8), 4411–4416. http://dx.doi.org/10.1063/1.325494.

Anderson O.L., Isaak D.G., 1995. Elastic constants of mantle minerals at high temperature. In: T.J. Ahrens (Ed.), Mineral physics and crystallography. A Handbook of Physical Constants. AGU Reference Shelf 2. AGU, Washington, p. 64–97. http://dx.doi.org/10.1029/RF002p0064.

Archer D.G., 1993. Thermodynamic properties of synthetic sapphire (α-Al_2O_3), standard reference material 720 and the effect of temperature-scale differences on thermodynamic properties. *Journal of Physical and Chemical Reference Data* 22 (6), 1441–1453. http://dx.doi.org/10.1063/1.555931.

Aristova N.M., Gusarov A.V., 2008. ChemNet. Available from: http://www.chem.msu.su/Zn/Cr/welcome.html (last accessed July 14, 2016).

Brosh E., Shneck Z., Makov G., 2008. Explicit Gibbs free energy equation of state for solids. *Journal of Physics and Chemistry of Solids* 69 (8), 1912–1922. http://dx.doi.org/10.1016/j.jpcs.2008.01.019.

Brown M.J., 1999. The NaCl pressure standard. *Journal of Applied Physics* 86 (10), 5801–5808. http://dx.doi.org/10.1063/1.371596.

Bruce R.H., Cannel D.S., 1977. Specific heat of Cr_2O_3 near the Neel temperature. *Physical Review B* 15 (9), 4451–4458. http://dx.doi.org/10.1103/PhysRevB.15.4451.

Chase M.W., 1998. NIST-JANAF thermochemical tables. Fourth Edition. Journal of Physical and Chemical Reference Data, Monograph 9. AIP, New York, 1951 p.

Chung D.H., Simmons G., 1968. Pressure and temperature dependences of the isotropic elastic moduli of polycrystalline alumina. *Journal of Applied Physics* 39 (11), 5316–5326. http://dx.doi.org/10.1063/1.1655961.

Decker D.L., 1971. High-pressure equation of state for NaCl, KCl, and CsCl. *Journal of Applied Physics* 42 (8), 3239–3244. http://dx.doi.org/10.1063/1.1660714.

Dera P., Lavina B., Meng Y., Prakapenka V.B., 2011. Structural and electronic evolution of Cr_2O_3 on compression to 55 GPa. *Journal of Solid State Chemistry* 184 (11), 3040–3049. http://dx.doi.org/10.1016/j.jssc.2011.09.021.

Dewaele A., Torrent M. 2013. Equation of state of α-Al_2O_3. *Physical Review B* 88 (6), 064107. http://dx.doi.org/10.1103/PhysRevB.88.064107.

Dinsdale A.T., 1991. SGTE data for pure elements. *CALPHAD* 15 (4), 317–425. http://dx.doi.org/10.1016/0364-5916(91)90030-N.

Dorogokupets P.I., 1995. Equation of state for lambda transition in quartz. *Journal of Geophysical Research* 100 (B5), 8489–8499. http://dx.doi.org/10.1029/94JB02917.

Dorogokupets P.I., 2010. *P-V-T* equations of state of MgO and thermodynamics. *Physics and Chemistry of Minerals* 37 (9), 677–684. http://dx.doi.org/10.1007/s00269-010-0367-2.

Dorogokupets P.I., Dewaele A., 2007. Equations of state of MgO, Au, Pt, NaCl-B1, and NaCl-B2: Internally consistent high-temperature pressure scales. *High Pressure Research* 27 (4), 431–446. http://dx.doi.org/10.1080/08957950701659700.

Dorogokupets P.I., Dymshits A.M., Sokolova T.S., Danilov B.S., Litasov K.D., 2015. The equations of state of forsterite, wadsleyite, ringwoodite, akimotoite, $MgSiO_3$-perovskite, and postperovskite and phase diagram for the Mg_2SiO_4 system at pressures of up to 130 GPa. *Russian Geology and Geophysics* 56 (1–2), 172–189. http://dx.doi.org/10.1016/j.rgg.2015.01.011.

Dorogokupets P.I., Oganov A.R., 2007. Ruby, metals, and MgO as alternative pressure scales: A semiempirical description of shock-wave, ultrasonic, x-ray, and thermochemical data at high temperatures and pressures. *Physical Review B* 75 (2), 024115. http://dx.doi.org/10.1103/PhysRevB.75.024115.

Dorogokupets P.I., Ponomarev E.M., Melekhova E.A., 1999. Optimization of experimental data on the heat capacity, volume, and bulk moduli of minerals. *Petrology* 7 (6), 574–591.

Dorogokupets P.I., Sokolova T.S., Danilov B.S., Litasov K.D., 2012. Near-absolute equations of state of diamond, Ag, Al, Au, Cu, Mo, Nb, Pt, Ta, and W for quasi-hydrostatic conditions. *Geodynamics and Tectonophysics* 3 (2), 129–166 (in Russian) [*Дорогокупец П.И., Соколова Т.С., Данилов Б.С., Литасов К.Д.* Почти абсолютные уравнения состояния алмаза, Ag, Al, Au, Cu, Mo, Nb, Pt, Ta, W для квазигидростатических условий // *Геодинамика и тектонофизика*. 2012. Т. 3. № 2. С. 129–166]. http://dx.doi.org/10.5800/GT-2012-3-2-0067.

Dorogokupets P.I., Sokolova T.S., Litasov K.D., 2014. Thermodynamic properties of bcc-Fe to melting temperature and pressure to 15 GPa. *Geodynamics and Tectonophysics* 5 (4), 1033–1044 (in Russian) [*Дорогокупец П.И., Соколова Т.С., Литасов К.Д.* Термодинамические свойства bcc-Fe до температуры плавления и до давления 15 ГПа // *Геодинамика и тектонофизика*. 2014. Т. 5. № 4. С. 1033–1044]. http://dx.doi.org/10.5800/GT-2014-5-4-0166.

Dubrovinskaya N.A., Dubrovinsky L.S., Saxena S.K., 1997. Systematics of thermodynamic data on solids: Thermochemical and pressure-volume-temperature properties of some minerals. *Geochimica et Cosmochimica Acta* 61 (19), 4151–4158. http://dx.doi.org/10.1016/S0016-7037(97)00233-0.

Dubrovinsky L.S., Saxena S.K., Lazor P., 1998. High-pressure and high-temperature in situ X-ray diffraction study of iron and corundum to 68 GPa using an internally heated diamond anvil cell. *Physical and Chemistry of Minerals* 25 (6), 434–441. http://dx.doi.org/10.1007/s002690050133.

Dymshits A.M., Dorogokupets P.I., Sharygin I.S., Litasov K.D., Shatskiy A., Rashchenko S.V., Ohtani E., Suzuki A., Higo Y., 2016. Thermoelastic properties of chromium oxide Cr_2O_3 (eskolaite) at high pressures and temperatures. *Physics and Chemistry of Minerals* 43 (6), 447–458. http://dx.doi.org/10.1007/s00269-016-0808-7.

Finger L.W., Hazen R.M., 1978. Crystal structure and compression of ruby to 46 kbar. *Journal of Applied Physics* 49 (12), 5823–5826. http://dx.doi.org/10.1063/1.324598.

Finger L.W., Hazen R.M., 1980. Crustal structure and isothermal compression of Fe_2O_3, Cr_2O_3, and V_2O_3 to 50 kbars. *Journal of Applied Physics* 51 (10), 5362–5367. http://dx.doi.org/10.1063/1.327451.

Funamori N., Jeanloz R., 1997. High-pressure transformation of Al_2O_3. *Science* 278 (5340), 1109–1111. http://dx.doi.org/10.1126/science.278.5340.1109.

Gatta G.D., Kantor I., Ballaran T.B., Dubrovinsky L., McCammon C., 2007. Effect of non-hydrostatic conditions on the elastic behavior of magnetite: an in situ single-crystal X-ray diffraction study. *Physical and Chemistry of Minerals* 34 (9), 627–635. http://dx.doi.org/10.1007/s00269-007-0177-3.

Gerya T.V., Maresch W.V., Podlesskii K.K., Perchuk L.L., 2004. Semi-empirical Gibbs free energy formulations for minerals and fluids for use in thermodynamic databases of petrological interest. *Physics and Chemistry of Minerals* 31 (7), 429–455. http://dx.doi.org/10.1007/s00269-004-0409-8.

Gerya T.V., Podlesskii K.K., Perchuk L.L., Swamy V., Kosyakova N.A., 1998. Equations of state of minerals for thermodynamic databases used in petrology. *Petrology* 6 (6), 511–526.

Goto T., Anderson O.L., Ohno I., Yamamoto S., 1989. Elastic constants of corundum up to 1825 K. *Journal of Geophysical Research* 94 (B6), 7588–7602. http://dx.doi.org/10.1029/JB094iB06p07588.

Grevel K.-D., Burchard M., Fabhauer D.F., 2000. Pressure-volume-temperature behavior of diaspore and corundum: An in situ X-ray diffraction study comparing different pressure media. *Journal of Geophysical Research* 105 (B12), 27877–27887. http://dx.doi.org/10.1029/2000JB900323.

Gronvold F., Samuelsen E.J., 1975. Heat capacity and thermodynamic properties of α-Fe_2O_3 in the region 300–1050 K. Antiferromagnetic transition. *Journal of Physics and Chemistry Solids* 36 (4), 249–256. http://dx.doi.org/10.1016/0022-3697(75)90017-7.

Gronvold F., Sveen A., 1974. Heat capacity and thermodynamic properties of synthetic magnetite (Fe_3O_4) from 300 to 1050 K. Ferrimagnetic transition and zero-point entropy. *Journal of Chemistry Thermodynamics* 6 (9), 859–872. http://dx.doi.org/10.1016/0021-9614(74)90230-4.

Gronvold F., Westrum E.F., 1959. α-Ferric Oxide: low temperature heat capacity and thermodynamic functions. *Journal of the American Chemical Society* 81 (8), 1780–1783. http://dx.doi.org/10.1021/ja01517a002.

Gurevich V.M., Kuskov O.L., Smirnova N.N., Gavrichev K.S., Markin A.V., 2009. Thermodynamic functions of eskolaite Cr_2O_3(c) at 0–1800 K. *Geochemistry International* 47 (12), 1170–1179. http://dx.doi.org/10.1134/S0016702909120027.

Gurvich L.V., Veits I.V., Medvedev V.A., 1981. Thermodynamic Properties of Substances. Vol. 3. Nauka, Moscow, 400 p. (in Russian) [*Гурвич Л.В., Вейц И.В., Медведев В.А.* Термодинамические свойства индивидуальных веществ. М.: Наука, 1981. Т. 3. 400 с.].

Hemingway B.S., 1990. Thermodynamic properties for bunsenite, NiO, magnetite, Fe_3O_4, and hematite, Fe_2O_3 with comments on selected oxygen buffer reactions. *American Mineralogist* 75 (7–8), 781–790.

Hill A.H., Harrison A., Dickinson C., Zhou W., Kockelmann W., 2010. Crystallographic and magnetic studies of mesoporous eskolaite, Cr_2O_3. *Microporous and Mesoporous Materials* 130 (1–3), 280–286. http://dx.doi.org/10.1016/j.micromeso.2009.11.021.

Holland T.J.B., Powell R., 2011. An improved and extended internally consistent thermodynamic dataset for phases of petrological interest, involving a new equation of state for solids. *Journal of Metamorphic Geology* 29 (3), 333–383. http://dx.doi.org/10.1111/j.1525-1314.2010.00923.x.

Ito E., Fukui H., Katsura T., Yamazaki D., Yoshino T., Aizawa Y., Kubo A., Yokoshi S., Kawabe K., Zhai S., Shatzkiy A., Okube M., Nozawa A., Funakoshi K.-I., 2009. Determination of high-pressure phase equilibria of Fe_2O_3 using the Kawai-type apparatus equipped with sintered diamond anvils. *American Mineralogist* 94 (2–3), 205–209. http://dx.doi.org/10.2138/am.2009.2913.

Jacobs M.H.G., Oonk H.A.J., 2001. The Gibbs energy formulation of the α, β, and γ forms of Mg_2SiO_4 using Grover, Getting and Kennedy's empirical relation between volume and bulk modulus. *Physics and Chemistry of Minerals* 28 (8), 572–585. http://dx.doi.org/10.1007/s002690100180.

Jacobs M.H.G, Schmid-Fetzer R., 2010. Thermodynamic properties and equation of state of fcc aluminum and bcc iron, derived from a lattice vibrational method. *Physics and Chemistry of Minerals* 37 (10), 721–739. http://dx.doi.org/10.1007/s00269-010-0371-6.

Jacobs M.H.G, Schmid-Fetzer R., Berg A.P., 2013. An alternative use of Kieffer's lattice dynamics model using vibrational density of states for constructing thermodynamic databases. *Physics and Chemistry of Minerals* 40 (3), 207–227. http://dx.doi.org/10.1007/s00269-012-0562-4.

Jephcoat A.P., Hemley R.J., Mao H.K., 1988. X-ray diffraction of ruby (Al_2O_3:Cr^{3+}) to 175 GPa. *Physica B+C* 150 (1–2), 115–121. http://dx.doi.org/10.1016/0378-4363(88)90112-X.

Kantor A., Kantor I., Merlini M., Glazyrin K., Prescher C., Hanfland M., Dubrovinsky L., 2012. High-pressure structural studies of eskolaite by means of single-crystal X-ray diffraction. *American Mineralogist* 97 (10), 1764–1770. http://dx.doi.org/10.2138/am.2012.4103.

Kim-Zajonz J., Werner S., Shultz H., 1999. High pressure single crystal X-ray diffraction study on ruby up to 31 GPa. *Zeitshrift fur Kristallographie* 214 (6), 331–336. http://dx.doi.org/10.1524/zkri.1999.214.6.331.

Kirby R.K., Hahn T.A., Rothrock B.D., 1972. Thermal expansion. In: B.H. Billings, D.E. Gray (Eds.), American Institute of Physics Handbook, 3rd edition. McGraw-Hill, New York, p. 4119–4142.

Klemme S., O'Neill H.S.C., Schnelle W., Gmelin E., 2000. The heat capacity of $MgCr_2O_4$, $FeCr_2O_4$, and Cr_2O_3 at low temperatures and derived thermodynamic properties. *American Mineralogist* 85 (11–12), 1686–1693. http://dx.doi.org/10.2138/am-2000-11-1212.

Lin J.-F., Degtyareva O., Prewitt C.T., Dera P., Sata N., Gregoryanz E., Mao H-K., Hemley R.J., 2004. Crystal structure of a high-pressure/high-temperature phase of alumina by in situ X-ray diffraction. *Nature Materials* 3 (6), 389–393. http://dx.doi.org/10.1038/nmat1121.

Liu Y., Oganov A.R., Wang S., Zhu Q., Dong X., Kresse G., 2015. Prediction of new thermodynamically stable aluminum oxides. *Scientific Reports* 5, 9518. http://dx.doi.org/10.1038/srep09518.

Logvinova A.M., Wirth R., Sobolev N.V., Seryotkin Y.V., Yefimova E.S., Floss C., Taylor L.A., 2008. Eskolaite associated with diamond from the Udachnaya kimberlite pipe, Yakutia, Russia. *American Mineralogist* 93 (4), 685–690. http://dx.doi.org/10.2138/am.2008.2670.

Moore G.E., Kelly K.K., 1944. High-temperature heat contents of the chromium carbides and chromic oxide. In: US Bureau of Mines Technical Report, vol. 662, p. 10–15.

Muan A., Sömiya S., 1959. Phase equilibrium studies in the system iron oxide-$A1_2O_3$-Cr_2O_3. *Journal of the American Ceramic Society* 42 (12), 603–613. http://dx.doi.org/10.1111/j.1151-2916.1959.tb13581.x.

Nakagiri N., Manghnani M.H., Ming L.C., Kimura S., 1986. Crystal structure of magnetite under pressure. *Physical and Chemistry of Minerals* 13 (4), 238–244. http://dx.doi.org/10.1007/BF00308275.

Oganov A.R., Ono S., 2005. The high-pressure phase of alumina and implications for Earth's D'' layer. *Proceedings of the National Academy of Sciences* 102 (31), 10828–10831. http://dx.doi.org/10.1073/pnas.0501800102.

Ono S., Ohishi Y., 2005. *In situ* X-ray observation of phase transformation in Fe_2O_3 at high pressures and high temperatures. *Journal of Physics and Chemistry of Solids* 66 (10), 1714–1720. http://dx.doi.org/10.1016/j.jpcs.2005.06.010.

Otero-de-la-Roza A., Luana V., 2011. Equations of state and thermodynamics of solids using empirical corrections in the quasiharmonic approximation. *Physical Review B* 84 (18), 184103. http://dx.doi.org/10.1103/PhysRevB.84.184103.

Pushcharovsky Yu.M., Pushcharovsky D.Yu., 2010. Geology of the Earth's Mantle. GEOS Publishing House, Moscow, 140 p. (in Russian) [*Пущаровский Ю.М., Пущаровский Д.Ю.* Геология мантии Земли. М.: ГЕОС, 2010. 140 с.].

Reichmann H.J., Jacobsen S.D., 2004. High-pressure elasticity of a natural magnetite crystal. *American Mineralogist* 89 (7), 1061–1066. http://dx.doi.org/10.2138/am-2004-0718.

Richet P., Xu J.-A., Mao H.-K., 1988. Quasi-hydrostatic compression of ruby to 500 kbar. *Physical and Chemistry of Minerals* 16 (3), 207–211. http://dx.doi.org/10.1007/BF00220687.

Ricolleau A., Fei Y., 2016. Equation of state of the high-pressure Fe_3O_4 phase and a new structural transition at 70 GPa. *American Mineralogist* 101 (3), 719–725. http://dx.doi.org/10.2138/am-2016-5409.

Robie R.A., Hemingway B.S., Fisher J.R., 1978. Thermodynamic Properties of Minerals and Related Substances at 298.15 K and 1 Bar Pressure and at Higher Temperatures. Washington, 456 p.

Sato Y., Akimoto S., 1979. Hydrostatic compression of four corundum-type compounds: α-Al_2O_3, V_2O_3, Cr_2O_3, and α-Fe_2O_3. *Journal of Applied Physics* 50 (8), 5285. http://dx.doi.org/10.1063/1.326625.

Saxena S.K., Shen G., 1992. Assessed data on heat capacity, thermal expansion and compressibility for some oxides and silicates. *Journal of Geophysical Research* 97 (B13), 19813–19825. http://dx.doi.org/10.1029/92JB01555.

Schauer A., 1965. Thermal expansion, Grueneisen parameter, and temperature dependence of lattice vibration frequencies of aluminum oxide. *Canadian Journal of Physics* 43 (4), 523–531. http://dx.doi.org/10.1139/p65-049.

Schultz A.H., Stubican V.S., 1970. Separation of phases by spinodal decomposition in the systems Al_2O_3-Cr_2O_3, and Al_2O_3-Cr_2O_3-Fe_2O_3. *Journal of the American Ceramic Society* 53 (11), 613–616. http://dx.doi.org/10.1111/j.1151-2916.1970.tb15984.x.

Shebanova O.N., Lazor P., 2003. Vibrational modeling of the thermodynamic properties of magnetite (Fe_3O_4) at high pressure from Raman spectroscopic study. *Journal of Chemical Physics* 119 (12), 6100–6110. http://dx.doi.org/10.1063/1.1602072.

Shim S-H., Duffy T.S., Jeanloz R., Yoo C.-S., Iota V., 2004. Raman spectroscopy and x-ray diffraction of phase transitions in Cr_2O_3 to 61 GPa. *Physical Review B* 69 (14), 144107. http://dx.doi.org/10.1103/PhysRevB.69.144107.

Sivasubramanian K., Raju S., Mohandas E., 2001. Estimating enthalpy and bulk modulus from thermal expansion data – a case study with α-Al_2O_3 and SiC. *Journal of the European Ceramic Society* 21 (9), 1229–1235. http://dx.doi.org/10.1016/S0955-2219(00)00323-X.

Skinner B.J., 1966. Section 6: Thermal expansion. In: S.P. Clark (Ed.), Handbook of Physical Constants. Geological Society of America Memoirs, vol. 97, p. 75–96. http://dx.doi.org/10.1130/MEM97-p75.

Snow C.L., Lee C.R., Shi Q., Boerio-Goates J., Woodfield B.F., 2010. Size-dependence of the heat capacity and thermodynamic properties of hematite (α-Fe_2O_3). *Journal of Chemical Thermodynamics* 42 (9), 1142–1151. http://dx.doi.org/10.1016/j.jct.2010.04.009.

Sokolova T.S., Dorogokupets P.I., Dymshits A.M., Danilov B.S., Litasov K.D., 2016. Microsoft excel spreadsheets for calculation of P-V-T relations and thermodynamic properties from equations of state of MgO, diamond and nine metals as pressure markers in high-pressure and high-temperature experiments. *Computers and Geosciences* 94, 162–169. http://dx.doi.org/10.1016/j.cageo.2016.06.002.

Sokolova T.S., Dorogokupets P.I., Litasov K.D., 2013. Self-consistent pressure scales based on the equations of state for ruby, diamond, MgO, B2–NaCl, as well as Au, Pt, and other metals to 4 Mbar and 3000 K. *Russian Geology and Geophysics* 54 (2), 181–199. http://dx.doi.org/10.1016/j.rgg.2013.01.005.

Stixrude L., Lithgow-Bertelloni C., 2005. Thermodynamics of mantle minerals – I. Physical properties. *Geophysical Journal International* 162 (2), 610–632. http://dx.doi.org/10.1111/j.1365-246X.2005.02642.x.

Strässle T., Klotz S., Kunc K., Pomjakushin V., White J.S., 2014. Equation of state of lead from high-pressure neutron diffraction up to 8.9 GPa and its implication for the NaCl pressure scale. *Physical Review B* 90 (1), 014101. http://dx.doi.org/10.1103/PhysRevB.90.014101.

Tucek J., Machala L., Ono S., Namai A., Yoshikiyo M., Imoto K., Tokoro H., Ohkoshi S., Zboril R., 2015. Zeta-Fe_2O_3 – A new stable polymorph in iron(III) oxide family. *Scientific Reports* 5, 15091. http://dx.doi.org/10.1038/srep15091.

Umemoto K., Wentzcovitch R.M., 2008. Prediction of an U_2S_3-type polymorph of Al_2O_3 at 3.7 Mbar. *Proceedings of the National Academy of Sciences* 105 (18), 6526–6530. http://dx.doi.org/10.1073/pnas.0711925105.

Vinet P., Ferrante J., Rose J.H., Smith J.R., 1987. Compressibility of solids. *Journal of Geophysical Research* 92 (B9), 9319–9325. http://dx.doi.org/10.1029/JB092iB09p09319.

Wachtman J.B., Scuderi T.G., Gleek G.W., 1962. Linear thermal expansion of aluminum oxide and thorium oxide from 100 to 1100 K. *Journal of the American Ceramic Society* 45 (7), 319–323. http://dx.doi.org/10.1111/j.1151-2916.1962.tb11159.x.

Wessel C., Dronskowski R., 2013. A first-principles study on chromium sesquioxide, Cr_2O_3. *Journal of Solid State Chemistry* 199, 149–153. http://dx.doi.org/10.1016/j.jssc.2012.12.019

Westrum E.F., Gronvold F., 1969. Magnetite (Fe_3O_4) heat capacity and thermodynamic properties from 5 to 350 K, low-temperature transition. *Journal of Chemical Thermodynamics* 1 (6), 543–557. http://dx.doi.org/10.1016/0021-9614(69)90015-9.

White G.K., Roberts R.B., 1983. Thermal expansion of reference materials: Tungsten and α-Al_2O_3. *High Temperatures. High Pressures* 15 (3), 321–328.

Wilburn D.R., Bassett W.A., Sato Y., Akimoto S., 1978. X ray diffraction compression studies of hematite under hydrostatic, isothermal conditions. *Journal of Geophysical Research* 83 (B7), 3509–3512. http://dx.doi.org/10.1029/JB083iB07p03509.

Woodland A.B., Frost D.J., Trots D.M., Klimm K., Mezouar M., 2012. In situ observation of the breakdown of magnetite (Fe_3O_4) to Fe_4O_5 and hematite at high pressures and temperatures. *American Mineralogist* 97 (10), 1808–1811. http://dx.doi.org/10.2138/am.2012.4270.

Worlton T.G., Brugger R.M., Bennion R.B., 1968. Pressure dependence of the Néel temperature of Cr_2O_3. *Journal of Physics and Chemistry of Solids* 29 (3), 435–438. http://dx.doi.org/10.1016/0022-3697(68)90120-0.

Zharkov V.N., Kalinin V.A., 1971. Equations of State of Solids at High Pressures and Temperatures. Consultants Bureau, New York, 257 p.

Ziemniak S.E., Anovitz L.M., Castelli R.A., Porter W.D., 2007. Thermodynamics of Cr_2O_3, $FeCr_2O_4$, $ZnCr_2O_4$, and $CoCr_2O_4$. *Journal of Chemistry Thermodynamics* 39 (11), 1474–1492. http://dx.doi.org/10.1016/j.jct.2007.03.001.

Dorogokupets, Peter I., Doctor of Geology and Mineralogy, Head of Laboratory
Institute of the Earth's Crust, Siberian Branch of RAS
128 Lermontov street, Irkutsk 664033, Russia
✉ e-mail: dor@crust.irk.ru

Дорогокупец Петр Иванович, докт. геол.-мин. наук, зав. лабораторией
Институт земной коры СО РАН
664033, Иркутск, ул. Лермонтова, 128, Россия
✉ e-mail: dor@crust.irk.ru

Sokolova, Tatiana S., Candidate of Geology and Mineralogy, Researcher
Institute of the Earth's Crust, Siberian Branch of RAS
128 Lermontov street, Irkutsk 664033, Russia
Tel.: 8(3952)511680, e-mail: sokolovats@crust.irk.ru

Соколова Татьяна Сергеевна, канд. геол.-мин. наук, н.с.
Институт земной коры СО РАН
664033, Иркутск, ул. Лермонтова, 128, Россия
Тел.: 8(3952)511680, e-mail: sokolovats@crust.irk.ru

Dymshits, Anna M., Candidate of Geology and Mineralogy, Senior Researcher
V.S. Sobolev Institute of Geology and Mineralogy, Siberian Branch of RAS
3 Academician Koptyug ave., Novosibirsk 630090, Russia
Tel.: 8(3833)303581, e-mail: a.dymshits@gmail.com

Дымшиц Анна Михайловна, канд. геол.-мин. наук, с.н.с.
Институт геологии и минералогии им. В.С. Соболева СО РАН
630090, Новосибирск, пр. Академика Коптюга, 3, Россия
Тел.: 8(3833)303581, e-mail: a.dymshits@gmail.com

Litasov, Konstantin D., Doctor of Geology and Mineralogy, Chief Researcher, Professor of RAS
V.S. Sobolev Institute of Geology and Mineralogy, Siberian Branch of RAS
3 Academician Koptyug ave., Novosibirsk 630090, Russia
Tel.: 8(3833)332517; e-mail: klitasov@igm.nsc.ru

Литасов Константин Дмитриевич, докт. геол.-мин. наук, г.н.с., профессор РАН
Институт геологии и минералогии им. В.С. Соболева СО РАН
630090, Новосибирск, пр. Академика Коптюга, 3, Россия
Тел.: 8(3833)332517; e-mail: klitasov@igm.nsc.ru